

Practical Quadrupole Theory: Pre-filters

Randall E. Pedder

Ardara Technologies L.P., 9937 McClellan Street, North Huntingdon, PA 15642

(Poster presented at the 53rd ASMS Conference on Mass Spectrometry and Allied Topics, June 5 - 9, 2005)

In the previous four years' ASMS conferences (1, 2, 3, 4), the first four of this series of simple graphical introductions to quadrupole theory were presented. This fifth presentation in the series builds on that previous work, examining the theoretical basis and practical implications of the use of pre-filters coupled to analytical quadrupoles to improve transmission and abundance sensitivity. Calculated ion trajectories are used to illustrate ion motion, and calculated phase space acceptance ellipses are used to interpret experimental results. The goal of this work is to help build an intuitive understanding of how quadrupoles work, and more importantly, how to optimize the design of experiments involving quadrupoles.

I. INTRODUCTION

The fringing field between an RF/DC quadrupole and a DC entrance lens voltage forces ions to traverse through a region of instability before they reach the stable region inside the quadrupole mass filter.

In 1968, Brubaker (5) demonstrated that the use of RF-only pre-filters between the entrance lens and the RF/DC quadrupole can minimize this effect, improving absolute sensitivity, peak shape and resolution.

In this work, an experimental implementation of pre-filters is optimized, both in selecting the appropriate RF level to apply to the pre-filter, and in selecting the appropriate length for the pre-filter.

II. THE EXPERIMENT

An Ardara Technologies 12 mm pre-filter quadrupole mass filter probe assembly, operated at 1.2 MHz, was configured with an axial molecular beam ionizer and analog multiplier detector to measure spectra of perfluorotributylamine leaked into the chamber background.

Two different length pre-filters were installed into the probe assembly, and peak shape was monitored under various tuning conditions, focusing on the effects of ion energy through the pre-filter, and through the quadrupole on mass peak profiles.

Resolution / Transmission curves and peak shapes were monitored for these two configurations as well.

Ion trajectories were calculated via Runge-Kutta numerical integration of the Mathieu equation using, HyperIon, a Turbo Basic program originally developed

by the author some eighteen years ago at the University of Florida.

These ion trajectories were used to calculate pseudopotential well depth for an RF-only quadrupole at various RF voltages.

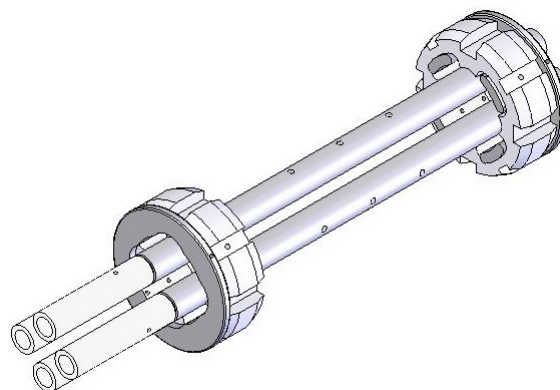


Figure 1. Model view of an eight inch long twelve mm rod diameter quadrupole with two inch long pre-filters.

III. QUADRUPOLE THEORY AND PRE-FILTERS

The traditional treatment of quadrupole theory starts with a derivation of the Mathieu equation from 'F=ma' all the way through to the final parameterized form, with the following parametric substitutions:

$$\frac{d^2u}{d\xi^2} + (a_u - 2q_u \cos 2\xi)u = 0 \quad a_u = \frac{8eU}{mr_0^2\Omega^2} \quad q_u = \frac{4eV}{mr_0^2\Omega^2}$$

The u in the above equations represents position along the coordinate axes (x or y), ξ is a parameter representing $\Omega t/2$, t is time, e is the charge on an electron, U is applied DC voltage, V is the applied zero-to-peak RF voltage, m is the mass of the ion, r is the effective radius between electrodes, and Ω is the applied RF frequency.

The family of solutions to this equation can be plotted in its parameterized form (a, q space) to become what is generally called the Mathieu stability diagram for a quadrupole. See figure 2.

Interpretation of this diagram is simple. Any a, q point within the stability diagram represents RF and DC voltages where the ion will have a stable (bounded) trajectory, and any point outside the stability diagram represents conditions where the ion trajectory will be rapidly pumped with energy by the quadrupolar field, resulting in an ion leaving the physical boundaries of the quadrupole.

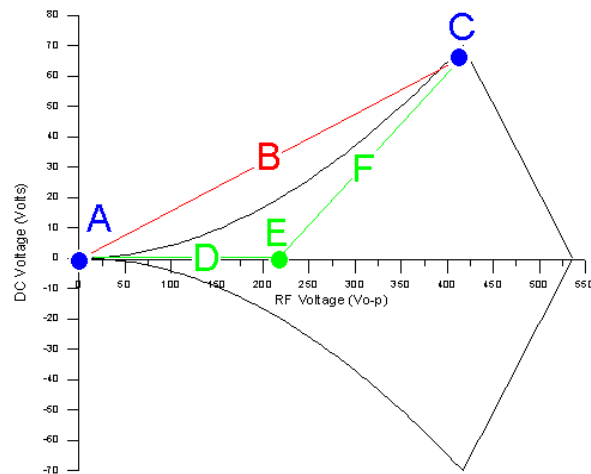


Figure 2. Mathieu stability diagram as calculated for m/z 502 for an 880 kHz 9.5 mm tri-filter.

Case 1: Entrance lens with RF-DC quadrupole:

A (entrance lens) -> B (gap, unstable region) -> C (quadrupole).

Case 2: Entrance lens with RF-only pre-filter, followed by RF-DC quadrupole:

A (entrance lens) -> D (gap) -> E (Pre-filter) -> F (gap) -> C (quadrupole). All stable.

Consider what happens when an ion enters a quadrupole through a DC voltage entrance lens. The ion leaves the space confined by DC lens voltages, and

is directed into an RF-DC quadrupole field, in which the ion has a theoretically stable trajectory.

The only problem is that in the space between the entrance lens and the quadrupole, the field is neither DC-only, nor is it the right ratio of RF to DC for stable trajectories, rather it is some combination thereof.

See figure 1 for a schematic view of an ion's path through a-q-space into the stability diagram, with and without the use of rf-only pre-filters.

With an entrance lens coupled with an RF-DC lens, ions travel from Point A (0 V RF and resolving DC) to Point C (just inside the tip of the stability diagram) through Region B (the gap between the entrance lens and the quadrupole, resulting in a symmetric DC lens voltage superimposed with quadrupolar RF and DC voltages), which is clearly outside the stability diagram. Ions traveling through a-q space along this path are either lost, or, at best, the surviving ions are accelerated radially to yield a wider cross sectional effective emittance area.

In contrast, with an rf-only pre-filter between the entrance lens and the quadrupole, ions travel from Point A (0 V RF and resolving DC) to Point C (just inside the tip of the stability diagram) through Region D (the gap between the entrance lens and the quadrupole, resulting in a symmetric DC lens voltage superimposed with quadrupolar RF-only voltages), through the pre-filter (Point E) and then through Point F, all of which points and regions are within the stability diagram, and yield stable trajectories.

In this way, the use of rf-only pre-filters between the entrance lens and the RF-DC quadrupole increases sensitivity, abundance sensitivity, and resolution. RF-only pre-filters have been called by many names through the years, including 'delayed d.c. ramp', Brubaker quadrupoles, and pre-filters.

Some manufacturers also include post-filters in their quadrupole designs.

IV. PHASE SPACE ACCEPTANCE ELLIPSES

One could use numerical methods to integrate the solution to of the Mathieu equation, yielding a family of solutions, which, when plotted in position-velocity space, illustrates the size of the sweet spot at the center of the quadrupole. (See reference 3 for a more detailed review of this method.)

Figure 3 represents the acceptance ellipses for an ion in an RF-only quadrupole for four different values of 'q'.

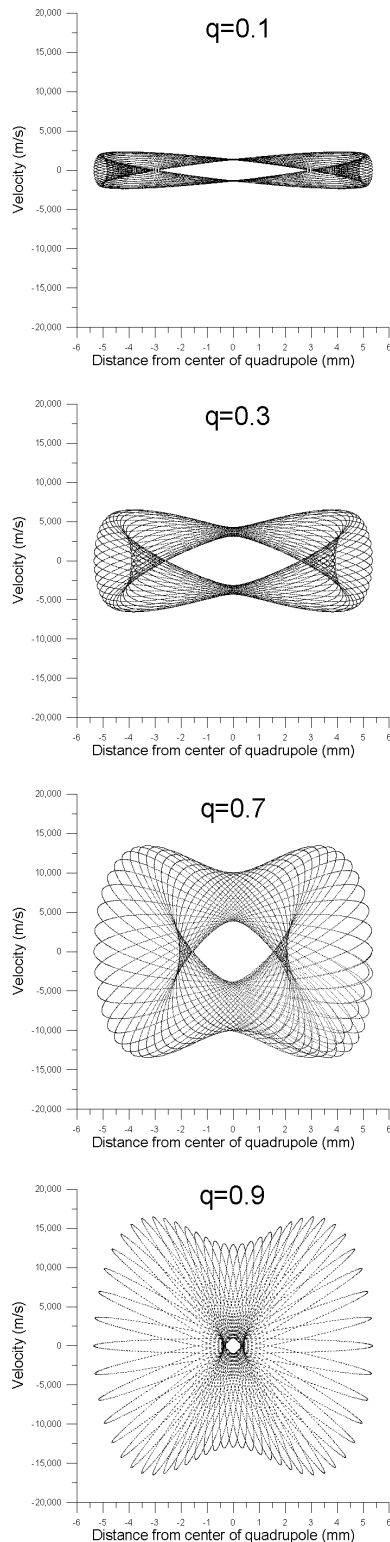


Figure 3. RF-only phase space diagrams for four different points on the Mathieu stability diagram, $q=0.1$, $q=0.3$, $q=0.7$, and $q=0.9$.

These diagrams can be interpreted such that if an ion falls on any point of one of the ellipses at its corresponding RF phase, it will be seen to process through all of the other ellipses, given enough time.

If an ion falls well within said ellipse for its instantaneous initial phase, then it will have a theoretically stable trajectory through the quadrupole, with a proportionally smaller set of ellipses.

What is interesting is that there is a sweet spot centered around the origin of the diagram, representing the superposition of all of the phase space acceptance ellipses. An ion injected into the quadrupole with minimal angle, and close to the center will have a stable trajectory through the quadrupole, regardless of RF phase. The span of this sweet spot in the positional direction represents the positional acceptance of the quadrupole.

The maximum velocity of these center acceptance ellipses can be used to represent the pseudopotential well depth, demonstrating the maximum ion energy that an ion can have and still be confined to the quadrupole.

Figure 4 represents the pseudopotential well depth for RF-only operation of a 12 mm quadrupole at 1.2 MHz at m/z 100. Note that pseudopotential well depth falls off at both low 'q' and at high 'q', with deepest wells at medium values of 'q'.

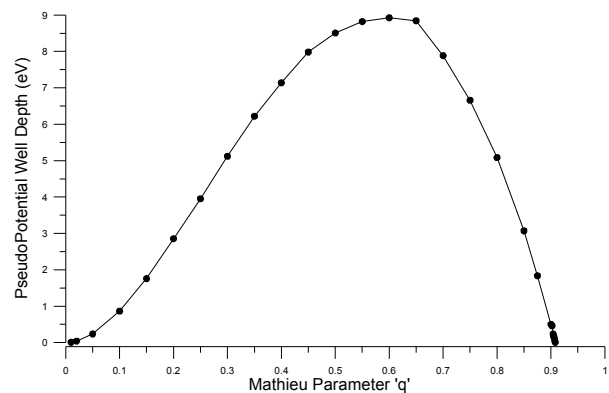


Figure 4. Pseudopotential Well depth for m/z 100 as a function of the Mathieu parameter 'q', with a 12 mm RF-only quadrupole operated at 1.2 MHz. Pseudopotential well depth is calculated based on the largest velocity that is within all RF phases in the phase space diagram.

V. RESISTOR SIZE SELECTION

A practical implementation of the addition of pre-filters to a quadrupole is to capacitively couple the pre-filter to the analytical quadrupole, utilizing the analytical RF power supply to power both the analytical quadrupole and the pre-filter.

The pole bias offset voltage is supplied to the capacitively coupled pre-filter through a pair of resistors, which serve to keep the RF from passing back through to the DC bias drive circuit. These pre-filter resistors also serve to control the fraction of the RF amplitude from the analytical quadrupole that gets applied to the pre-filters, in a sort of capacitive voltage divider.

In a series of experiments, relative amplitudes of a range of masses were measured with various pre-filter resistor sizes. Figure 5 represents this data set, illustrating that the optimum resistor size for higher masses tends to be lower than the optimum size for lower masses. If one chooses to use a very large resistor, tightly coupling the RF level on the pre-filter to approach the RF level on the analytical rods, then it is predicted that the system would be biased against higher masses.

It would be predicted that optimum transmission would coincide with maximum pseudopotential well depth, but the optimum RF-only transmission seems to be between a q of 0.3 and 0.4, while the optimum pseudopotential well depth is in the range of q of 0.5 to 0.7. Clearly there are other factors involved, including the positional acceptance of the quadrupole, as well as a phase shift that can occur at capacitor that is used to couple the RF from the analytical quadrupole to the pre-filter.

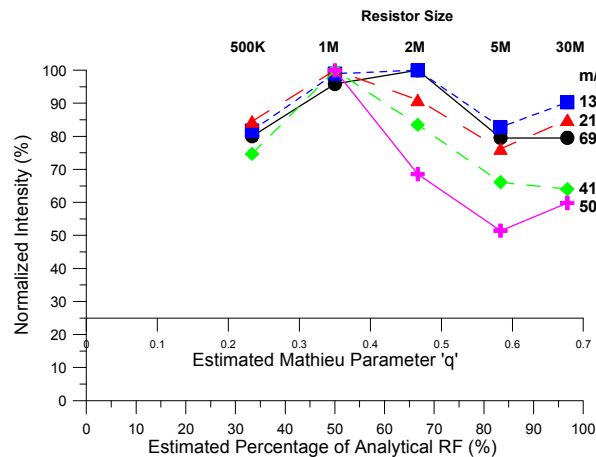


Figure 5. Experimentally measured intensities for different masses of perfluorotributylamine, for different pre-filter resistor sizes. Intensities for each mass were normalized to the largest intensity in a given series.

VI. PRE-FILTER LENGTH SELECTION

The effect of pre-filter length on performance was examined experimentally by using two different length pre-filter assemblies, 0.5 inches, and 2.0 inches.

It was found that the longer pre-filters yielded smoother tuning curves for pre-filter offset voltage (Figures 6 and 7), an also minimized the peak splitting at the top of the mass peak as ion energy is increased, allowing for higher ion energies through the analytical quadrupole, with commensurate increase in absolute sensitivity (Figures 8 and 9).

Figures 10 and 11 demonstrate the performance of the optimized quadrupole mass filter with pre-filters.

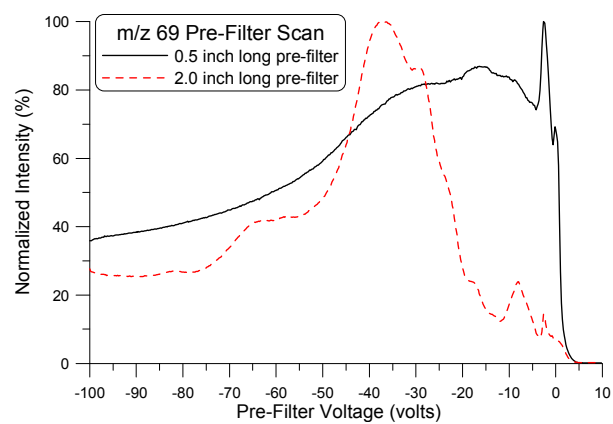


Figure 6. Pre-Filter scan for m/z 69 with short and long pre-filters. Note the narrow maximum for the shorter pre-filter, contrasts with the broader maximum for the longer pre-filter.

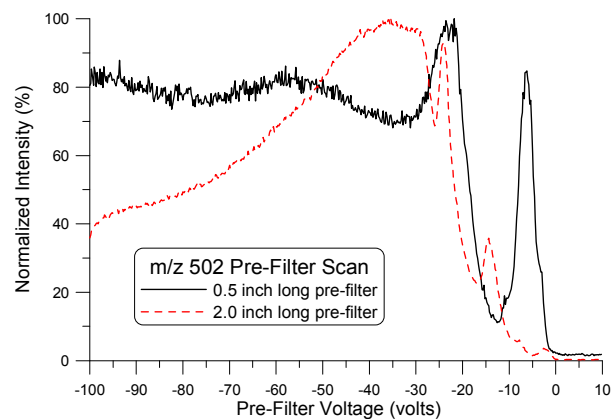


Figure 7. Pre-Filter scan for m/z 502 with short and long pre-filters.

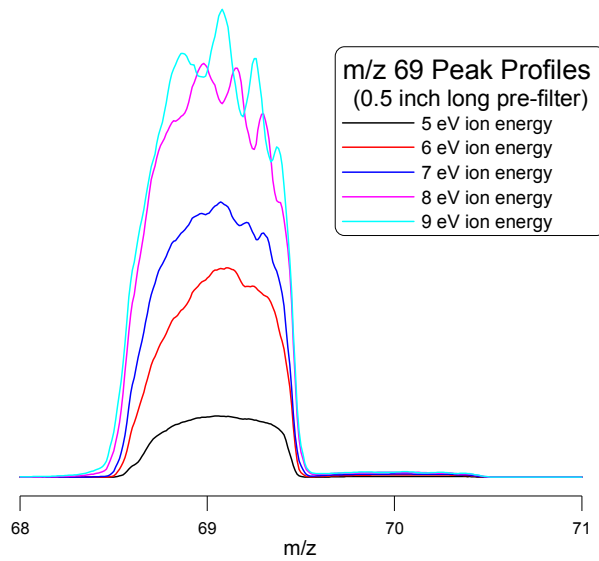


Figure 8. Peak profiles for m/z 69 at various ion energies for the shorter pre-filter. Note the dramatic splitting at the top of the peak as ion energy is increased with the shorter pre-filter.

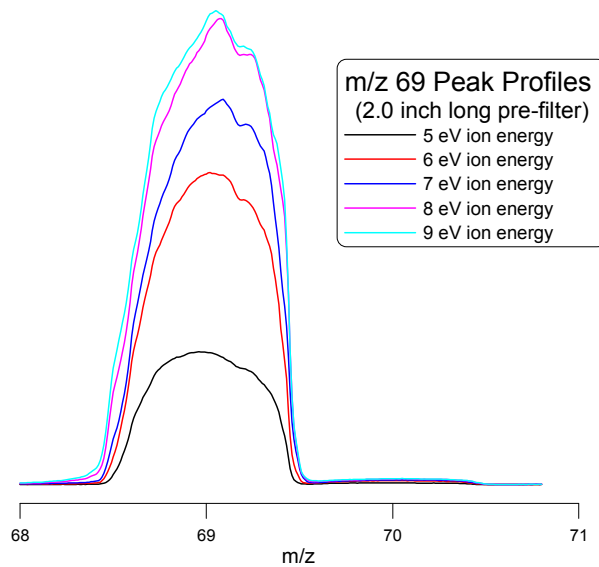


Figure 9. Peak profiles at various ion energies for the longer pre-filter. Note the absence of the dramatic splitting at the top of the peak as ion energy is increased, as was seen with the shorter pre-filter.

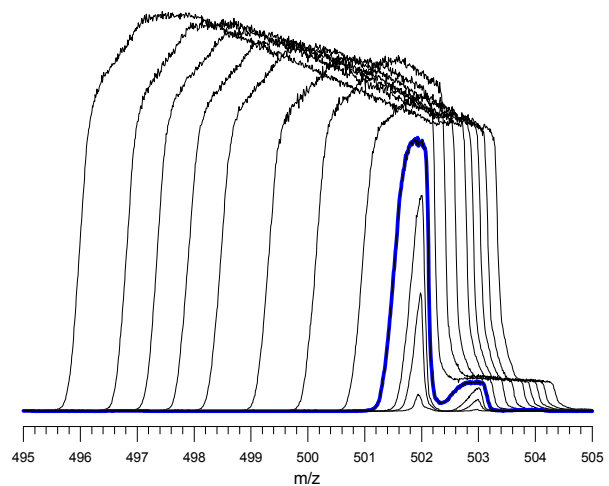


Figure 10. Family of peak shapes at various resolutions for m/z 502. The thick blue line shows ~68% relative transmission at unit mass resolution.

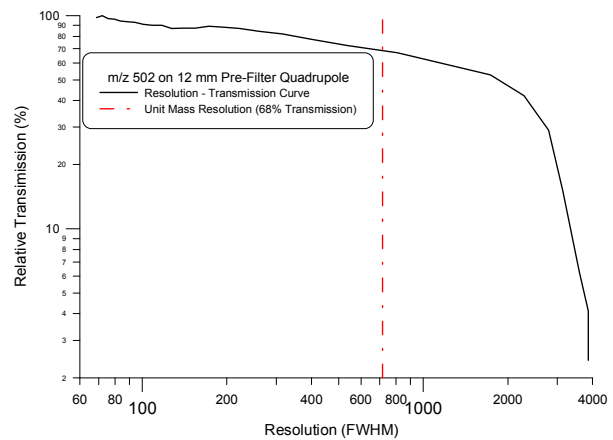


Figure 11. Resolution – Transmission curve for Ardara Technologies 12 mm quadrupole, showing relative transmissions of ~68% at unit mass resolution.

VII. CONCLUSIONS

Pseudopotential well depth for RF-only quadrupoles can be calculated from the velocity maxima of the acceptance ellipse at the center of a phase space acceptance ellipse diagram.

The use of pre-filters increases absolute sensitivity by minimizing the effects of fringing fields at the entrance to the quadrupole.

Longer pre-filters definitely provide smoother mass peak shapes compared to shorter pre-filters, allowing for higher ion energies with associated higher sensitivity.

Longer pre-filters also provide smoother tuning curves, making it easier to tune the system.

When using pre-filters, it is important to optimize the RF amplitude through appropriate resistor selection, to prevent mass discrimination.

VIII. REFERENCES

1. Pedder R.E. "*Practical Quadrupole Theory: Graphical Theory*", Extrel CMS, L.P. Application Note RA_2010A, Poster presented at the 49th ASMS Conference on Mass Spectrometry and Allied Topics, Chicago, IL, 2001.
2. Pedder R.E. "*Practical Quadrupole Theory: Peak Shapes at Various Ion Energies*", Extrel CMS, L.P. Application Note RA_2011A, Poster presented at the 50th ASMS Conference on Mass Spectrometry and Allied Topics, Orlando, FL, 2002.
3. Pedder R.E. "*Practical Quadrupole Theory: Quadrupole Emittance Characteristics*", Extrel CMS, L.P. Application Note RA_2012B, Poster presented at the 51st ASMS Conference on Mass Spectrometry and Allied Topics, Montreal Quebec Canada, 2003.
4. Pedder R.E. "*Practical Quadrupole Theory: Quadrupole Acceptance Characteristics*", Poster presented at the 52nd ASMS Conference on Mass Spectrometry and Allied Topics, Nashville, TN, 2004.
5. Brubaker, W.M., "*Advances in Mass Spectrometry*", 4 (1968) 293.

IX. ACKNOWLEDGEMENTS

The author would like to thank Jim Gauss, Brian Novak, Larry Pedder, and Mike Tusay for their contributions to this work.